Sediment entrainment under fully developed waves as a function of water depth, boundary layer thickness, bottom slope and roughness

J.P. Le Roux

Departamento de Geología, Facultad de Ciencias Físicas y Matemáticas, Universidad de Chile, Casilla 13518, Correo 21, Santiago, Chile

ARTICLE INFO

ABSTRACT

Many sediment entrainment equations for oscillatory waves are based on the linear (Airy) theory for deep water, but at the depth where such waves begin to transport sediments they commonly have trochoidal or cnoidal (non-linear) forms. These changes in the wave profile, together with the fact that it is displaced upward with respect to the still water level (SWL), have a profound influence on the hydrodynamics. A method is presented to determine the thickness of the boundary layer from the wave profile, which can be used to calculate the boundary velocity under the wave crest and trough, respectively, in any water depth. The critical boundary velocity can be determined from a published procedure based on laboratory experiments that takes account of the sediment and water properties as well as the wave period. An adjustment is made for the bottom slope and roughness, so that differential land- or seaward sediment entrainment can be predicted for any defined wave cycle. The results explain why sediments are normally transported landward under fair weather conditions and seaward during storms.

© 2009 Elsevier B.V. All rights reserved.

1. Introduction

Sediment transport by waves commences when fluid flow forces such as shear stress exceed the resisting forces such as gravity and bottom friction (Van Rijn, 2007). In unidirectional currents, the shear stress is normally determined by measuring flow velocity profiles (Middleton and Southard, 1984), but under waves only the water particle velocity at the top of the boundary layer is measured at the moment of entrainment, which is known as the critical boundary velocity U_{wle}. The top of the boundary layer is defined as the level where the vertical component of water particle motion below the waves reduces to zero so that only the horizontal component remains (Fig. 1).

Although U_{wle} can be measured under laboratory conditions, its determination in the field is generally impractical. A major obstacle is that the exact thickness of the boundary layer (δ) is unknown, so that the depth at which the horizontal particle velocity should be measured cannot be determined accurately. This is especially true of non-linear waves where δ depends on the wave profile and its position relative to the still water level (SWL).

In an attempt to find a solution to this problem, recent advances in wave modeling (Le Roux, 2007a,b, 2008a,b) are analyzed here, based on the following concepts:

— The horizontal water particle velocity can be calculated at any depth z from the SWL in deep water or below the displaced water level (DWL) in shallow water (Le Roux, 2008a), so that the actual boundary velocity U_{wl} can be determined if DWL and δ are known.
— Methods based on published laboratory data (e.g. Bagnold, 1946; Manohar, 1955; Rance and Warren, 1969; Komar and Miller, 1973; Migniot, 1977; White, 1989; Le Roux, 2001; You and Yin, 2006) can be used to determine the critical boundary velocity required to entrain sediments of different sizes and densities.
— To obtain the water depth at which sediment entrainment will commence under any specific wave condition, the water depth can be iterated until the boundary velocity U_{wl} coincides with the critical boundary velocity U_{wle}.

Only the case of fully developed deepwater waves propagating into shallow water is discussed here, because developing deepwater waves have different characteristics that cannot be modeled by linear or other existing theories. In particular, such waves are shorter and steeper with profiles somewhat similar to shallow water waves, so that their hydrodynamic properties deviate significantly from those of fully developed waves.

2. Two key concepts

2.1. Wave profile

The profile of waves as they propagate into shallow water has a significant influence on their hydrodynamic properties. As they shoal, the wave crests become more peaked while the troughs flatten out, their shape thus changing from sinusoidal to trochoidal and finally

E-mail address: jroux@ing.uchile.cl.
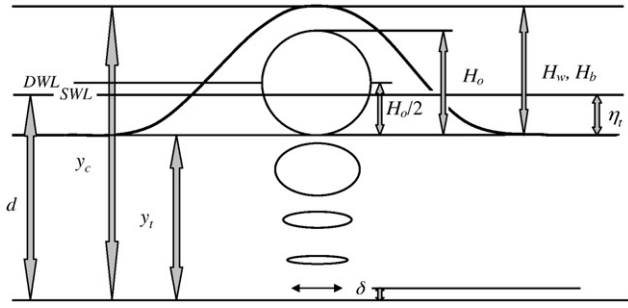
Fig. 1. Non-linear wave profile defining some symbols used in the text.

cnoidal just before breaking (Boussinesq, 1871; Korteweg and De Vries, 1895).

Le Roux (2008b) proposed the following equation that is valid for all water depths (using radians):

$$\eta(x) = L_w \left[D \cos \frac{2\pi x}{L_w} + \pi^2 D^4 f \cos \frac{4\pi x}{L_w} \right] \tag{1}$$

where $\eta(x)$ is the water surface elevation above or below the SWL at any point x, which is the distance from the wave crest in the direction of wave propagation, L_w is the wavelength (the subscript $_w$ indicating any water depth), $D = 0.017683$ for fully developed waves, and f is given by

$$f = \left[\frac{\left(2 + \cosh \frac{4\pi d}{L_w} \right) \cosh \frac{2\pi d}{L_w}}{2 \left(\sinh \frac{2\pi d}{L_w} \right)^3} \right]^3 . \tag{2}$$

In deep water, where $f = 1$, Eq. (1) yields a sinusoidal profile exactly the same as that given by linear wave theory (Airy, 1845), but in shallow water it models the change from a trochoidal to cnoidal form, as well as the upward displacement of the wave profile relative to the SWL.

Eq. (1) provides the basic wave profile, but requires an adaptation for the crest, adding the height derived from Eq. (14) below to the trough elevation (see Le Roux, 2008b, noting that Eq. (7) in that paper should read $\eta = \left[\frac{\eta_p}{\left(\eta_{pc} / \eta_c \right)^i} \right]$).

In sediment transport only the trough elevation η_t below the SWL is important, which can be simplified to

$$\eta_t = L_w (-0.017638 + 9.64 \times 10^{-7} f). \tag{3}$$

2.2. Median crest and trough diameter

To model water particle velocities below the wave crest and trough, respectively, Le Roux (2008a) introduced the concept of the median crest diameter (MCD) and median trough diameter (MTD), which are here redefined (Fig. 1) as the distance between the wave flanks under the crest and above the trough, respectively, at a level halfway between the trough and a distance of H_o above the trough (H_o being the deepwater wave height).

At the surface, water particles follow a circular path. With distance from the surface in shallow water, however, the orbits become ellipses of increasing elongation until the motion is only to and fro. The level where the vertical component of particle displacement or the semi-excursion reduces to zero is the top of the boundary layer.

Above and below the level of the MCD, water particle motion is landward and seaward, respectively. In shallow water waves, where the MCD is much shorter than the MTD, the time available for the water particles to complete the half-orbit above the MCD is much less than the time to complete the half-orbit below the MTD. It follows

that the water particle velocity must be significantly higher under the wave crest than under the trough.

The median crest diameter MCD_w in any water depth is calculated by (Le Roux, 2008a):

$$MCD_w = L_w - \frac{L_o}{2} \tag{4}$$

where the subscript $_o$ indicates deepwater conditions.

MCD_w reaches a minimum value of $\frac{L_o}{6}$ over any bottom slope, whereas the median trough diameter MTD_w is obtained from

$$MTD_w = \frac{L_o}{2} = \frac{gT_w^2}{4\pi} . \tag{5}$$

Eq. (5) is valid up to the breaking depth d_b (the subscript $_b$ indicating conditions at breaking) over a nearly horizontal bottom, but decreases into water shallower than this depth over sloping bottoms, in which case it is given by

$$MTD_w = L_w - \frac{L_o}{6} . \tag{6}$$

The MCD and MTD can be used to calculate the horizontal (A_{whz}) and vertical (A_{wvz}) maximum water particle displacement or semi-excursion at any depth z from the SWL (Le Roux, 2008a, correcting an error in that publication):

$$A_{whz} = \frac{H_o}{2} \left[\frac{\cosh \frac{\pi(d-z)}{MCD_w}}{\cosh \frac{\pi d}{MCD_w}} \right] \tag{7}$$

and

$$A_{wvz} = \frac{H_o}{2} \left[\frac{\sinh \frac{\pi(d-z)}{MCD_w}}{\sinh \frac{\pi d}{MCD_w}} \right] . \tag{8}$$

Eqs. (7) and (8) model both the horizontal and vertical semi-excursion to be $0.5 H_o$ at the surface in any water depth, in contrast to most textbooks that show an elliptic path in shallow water. However, photographs visualizing the flow paths (see Fig. 9.6 of Leeder, 1999, taken from Van Dyke, 1982) confirm that the orbital motion is actually circular at the surface, but rapidly flattens out with distance below the DWL.

The water particle semi-excursions are used to compute the horizontal velocity under the wave crest (U_{whcz}) and trough (U_{whtz}) at any depth z from the SWL or DWL (Le Roux, 2008a):

$$U_{whcz} = \frac{A_{whz} g T_w L_w}{4 MCD_w^2} \tag{9}$$

and

$$U_{whtz} = \frac{A_{whz} g T_w L_w}{4 MTD_w^2} . \tag{10}$$

3. Wave characteristics and water particle velocities in deep water

To calculate the hydrodynamics of a wave in shallow water, its deepwater characteristics are required. Fully developed deepwater waves are sinusoidal in shape and can be modeled using classical linear wave theory combined with some recent equations (Le Roux, 2008a). The length of such waves L_o is given by the standard expression (Airy, 1845):

$$L_o = \frac{gT_w^2}{2\pi} \tag{11}$$

where g is the acceleration due to gravity (9.81 m s^{-2}).

The fully developed deepwater wave height (H_o) can be found by (Le Roux, 2008a):

$$H_o = \frac{gT_w^2}{18\pi^2} \tag{12}$$

where the T_w is obtained from the wind velocity U_a as follows (Le Roux, 2008a):

$$T_w = \frac{2\pi U_a}{g}. \tag{13}$$

In deep water, water particles below the wave crest and trough rotate in simple harmonic motion, defining circular trajectories with a decrease in orbital diameter as the distance below the still water level (z) increases. The orbital water particle velocity U_{oz} at any distance z below the SWL can be modeled using linear theory (Airy, 1845) or Eq. (9) or (10).

4. Wave characteristics and particle velocities in any water depth

As waves begin to shoal there is an initial, very gradual decrease in wave height, followed by a decrease in wavelength and eventually a fairly rapid increase in wave height up to the breaker zone. The wave profile also changes as mentioned above, which is accompanied by its upward displacement with respect to the SWL. The characteristics of such shoaling, non-linear waves have been modeled by many authors (e.g. Bretschneider, 1960; Latoine, 1960; Skjelbreia and Hendrickson, 1961; Chappelear, 1962; Latoine, 1962, 1965; Ippen, 1966; Peregrine, 1972; Cokelet, 1977; Phillips, 1977; Fenton, 1985; Chakrabarti, 1987; Fenton, 1988; Dean and Dalrymple, 1991; Mei, 1991). However, the simplified but fully integrated equations of Le Roux (2007a,b, 2008a,b) are used here, because they eliminate the discrepancies produced when using different wave theories for different water depths.

To model the wave hydrodynamics in water of any depth, the breaking depth d_b and breaker height H_b must be calculated first (Le Roux, 2007a). Eqs. (14) and (15) below are based on the 110th order wave theory of Cokelet (1977) and published laboratory data (Shore Protection Manual, 1984) for waves breaking over different bottom slopes.

Cokelet's (1977) theory models the height H_w of waves propagating into any water depth d and was simplified by Le Roux (2007a) to:

$$H_w = H_o\left[A\exp\left(\frac{H_o}{L_o}B\right)\right] \tag{14}$$

where $A = 0.5875\left(\frac{d}{L_o}\right)^{-0.18}$ when $\frac{d}{L_o} \leq 0.0844$; $A = 0.9672\left(\frac{d}{L_o}\right)^2 - 0.5013\left(\frac{d}{L_o}\right) + 0.9521$ when $0.0844 \leq \frac{d}{L_o} \leq 0.6$; $A = 1$ when $\frac{d}{L_o} > 0.6$; $B = 0.0042\left(\frac{d}{L_o}\right)^{-2.3211}$.

The bottom slope effect is modeled by

$$H_{b\alpha} = d_{b\alpha}(-0.0036\alpha^2 + 0.0843\alpha + 0.835) \tag{15}$$

where α is the slope angle.

The breaker height H_b and depth d_b are obtained by iterating d in Eqs. (14) and (15) until H_w coincides with $H_{b\alpha}$.

The breaker length $L_{b\alpha}$ can be found by (Le Roux, 2007b)

$$L_{b\alpha} = T_w\sqrt{g(0.5H_{b\alpha} + d_{b\alpha})}. \tag{16}$$

$L_{b\alpha}$ can be used in turn to calculate the wavelength L_w in any water depth (Le Roux, 2007b):

$$L_w = \sqrt{L_{b\alpha}T_w\sqrt{g(0.5H_{b\alpha} + d)}} \tag{17}$$

where d has a maximum value of $\frac{L_o}{2.965}$.

Once obtained, L_w can be used to calculate MCD_w and MTD_w (Eqs. (4)–(6)), and therewith the water particle velocity at any depth d and distance z from the SWL (Eqs. (9) and (10)).

5. Thickness of the boundary layer

Accurate measurement of the boundary layer thickness is difficult and the various equations give widely discrepant results. For example, Li (1954) calculated the thickness by

$$\delta = 6.5\sqrt{\frac{\mu T_w}{2\rho\pi}} \tag{18}$$

where μ and ρ are the dynamic viscosity and density of the water, respectively.

Wang (2007), following Jonsson (1966), determined δ from

$$\delta = \frac{A_{whl}}{30} \tag{19}$$

where A_{whl} is the horizontal water particle displacement at the top of the boundary layer.

However, the value of δ depends not only on the water properties and wave period, but also on the vertical water particle displacement (which must reach zero at this level) and the water depth. To calculate A_{wvl} from Eq. (7), z must be measured from the DWL and not from the SWL, which is at a distance d from the bottom. However, the DWL cannot be simply taken as halfway between the trough and crest. For example, when propagating into intermediate water depths the wave height initially decreases while the trough depth remains constant, so that a distance of $z = d$ below the DWL would lie below the sea floor if the DWL were to be taken as $\frac{y_c - y_t}{2}$, where y_c and y_t are the distances of the crest and trough from the bottom, respectively (see Fig. 1). This would mean that δ has a negative value, which is impossible. Just before breaking, however, the wave trough is displaced upward with respect to its deepwater level, so that the mean water surface must lie at some distance above $\frac{y_c - y_t}{2}$.

A solution to this problem is to take DWL as $0.5H_o$ above the trough. This corresponds to the SWL in deep water as it should, does not result in a negative value in intermediate depths, and lies above the $\frac{y_c - y_t}{2}$ level in shallow water.

Considering that $DWL = y_t + 0.5H_o$, Eq. (8) calculates the vertical water particle displacement to become zero at a certain distance from the bottom, which is here considered to represent the thickness of the boundary layer δ. This gives

$$\delta = \frac{H_o}{2} + \eta_t \tag{20}$$

η_t being a negative value according to Eq. (3).

Eq. (20) models a practically zero boundary layer thickness as the waves propagate from deep water up to a depth of $\frac{L_o}{2.965}$, from which point on it begins to increase. This is to be expected, because both f in Eq. (2) and thus η_t in Eq. (3) are directly related to L_w, which begins to decrease at this depth. The increase in δ is accompanied by an increase in the rate of flattening of the orbital paths below the circular water particle motion at the surface. Most probably, the upward displacement of the wave profile with respect to the SWL can be attributed to the growth of the boundary layer, which in turn would be related to increasing bottom friction.

Simplifying the relationships above, the boundary velocity under the wave crest U_{wlc} can be determined directly as follows:

$$U_{wlc} = \frac{H_o g T_w L_w}{8MCD_w^2 \cosh\frac{\pi d}{MCD_w}}. \tag{21}$$

Under the wave trough, the boundary velocity is obtained from

$$U_{wlt} = \frac{H_o g T_w L_w}{8 M T D_w^2 \cosh \frac{\pi d}{M C D_w}}. \tag{22}$$

It must be emphasized here that the obtained boundary velocities are peak values attained only momentarily during each wave cycle.

6. Sediment characteristics and critical boundary velocity

The critical boundary velocity required to entrain sediments of different sizes and densities under waves is derived from laboratory data. Fig. 2 compares 3 different methods (Komar and Miller, 1973, 1975; You and Yin, 2006) based on the data of Bagnold (1946), Manohar (1955), Rance and Warren (1969), and Hammond and Collins (1979). All these methods use the near-bed velocity and semi-excursion, or alternatively the wave period, together with the grain properties to calculate the critical boundary velocity. With this data set, the method of You and Yin (2006) produces the highest correlation coefficient R^2 of 0.9707 with the experimentally observed critical boundary velocities, compared with 0.9667 using Komar and Miller (1975) and 0.9210 using Komar and Miller (1973).
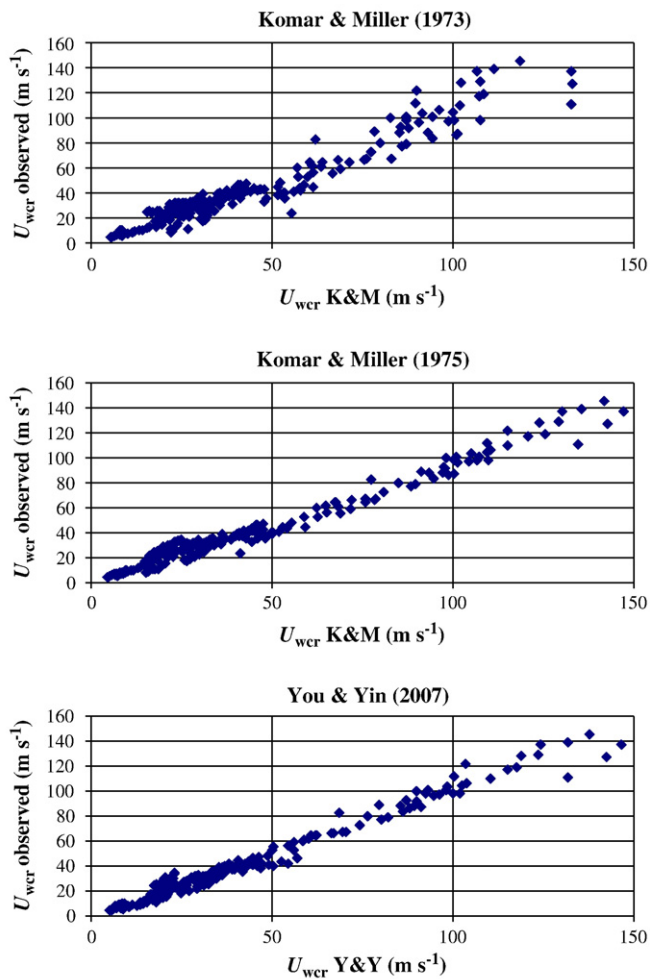
Fig. 2. Comparison of three different methods to estimate sediment entrainment under waves.
Data from Bagnold (1946), Manohar (1955), Rance and Warren (1969), and Hammond and Collins (1979).

You and Yin (2006) proposed the following approach to calculate the critical boundary velocity U_{wle} (all units in grams, centimeters and seconds):

$$U_{wle} = 2\pi C \left[1 + 5 \left(\frac{T_R}{T_w} \right)^2 \right]^{-1/4} \tag{23}$$

where T_w is the wave period, while C and T_R are coefficients derived from s_*, a scaled dimensionless immersed sediment weight given by:

$$s_* = \frac{D \sqrt{\rho_\gamma g D}}{4\upsilon} \tag{24}$$

υ being the kinematic viscosity of the water $\left(\frac{\mu}{\rho} \right)$. From s_*:

$$C = \frac{2.53 s_*^{0.92} \upsilon}{D} \tag{25}$$

and

$$T_R = \frac{159 s_*^{-1.3} D^2}{\upsilon}. \tag{26}$$

Le Roux (2007c) demonstrated that this method underestimates the critical boundary velocity when the latter exceeds 80 cm s^{-1}, and proposed the following correction:

$$U_{wle} = 1.5X - 40 \text{ when } X > 80 \tag{27}$$

where X is the U_{wle} value calculated by Eq. (23).

It is thus possible to obtain both the boundary velocity for fully developed waves propagating in any water depth over any bottom slope, and the critical boundary velocity required to entrain sediment of a given size and density in water with a specific density and viscosity. Iterating the water depth until these two values coincide under the wave crest and trough, respectively, therefore determines the respective depths where sediment entrainment commences.

7. Effect of bottom roughness and bed slope on sediment entrainment

Different authors (Allen, 1982; Dyer, 1986; Soulsby and Whitehouse, 1997; Le Roux, 2005) have investigated the relationship between entrainment thresholds and bed slope, but basically all methods can be reduced to

$$U_{wle\alpha} = 1.3934 U_{wle} \sqrt{\sin(\varphi + \alpha)} \tag{28}$$

where α is the bed slope in degrees and φ is the pivot angle between grains. The only difference among these authors is that different values were proposed for φ, e.g. 35° (Allen, 1982), 32° (Soulsby and Whitehouse, 1997), 31° (Le Roux, 2005), and 30° (Dyer, 1986).

Theoretically, there is a simple solution to this problem as shown in Fig. 3. In the case of perfect spheres, the line AB would always be perpendicular to CD, no matter what the difference in grain size, as long as half or more of the grain is exposed above the top of the underlying grains. In ΔGDC, $\varphi = \angle$BAC $= \angle$DGE. CD $=$ CF $+$ FD $= \frac{D_1}{2} + \frac{D_2}{2}$; and GC $=$ 2CE $= D_1$, where D_1 and D_2 are the sizes forming the bed roughness and grain being entrained, respectively. Therefore

$$\varphi = \arcsin \frac{D_1}{D_1 + D_2} \tag{29}$$

and the value of φ for perfect spheres of the same size would be 30°. The value of 1.3934 in Eq. (29) is derived from an angle of 31° (being given by $\frac{1}{\sqrt{\sin\varphi}}$), which is the experimental friction angle of well
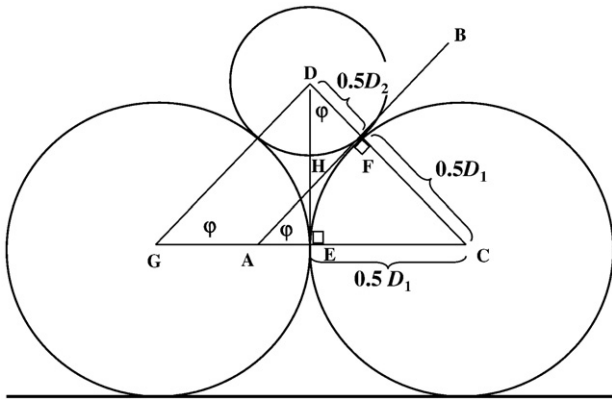
Fig. 3. Derivation of friction angle φ. D, G and C are the centerpoints of each grain, DC is perpendicular to the grain surfaces and AB is perpendicular to DC. The friction angle φ ($\angle$BAC) is equal to $\angle$DGC. In ΔEDC, $\varphi = \arcsin \frac{D_1}{D_1 + D_2}$, where D_1 and D_2 are the diameters of grains C and D, respectively.

sorted, well rounded sand (Whitehouse and Hardisty, 1988; Le Roux, 2005). Considering that most experiments on wave entrainment also use well sorted natural sand, a 31° angle is considered to be most appropriate as a base value. The maximum angle of φ is 53°, which is reached when less than half of the smaller grain is exposed above the tops of the bed roughness grains and remains so until the top of the smaller grain is level with the tops of the underlying grains.

8. Examples, practical applications and comparison with other wave theories

8.1. Deepwater waves

In the discussion below, the methodology is illustrated with the particular case of fully developed waves having a period of 5 s. Such 5 s waves would be generated by wind with a velocity of 7.81 m s^{-1} (Eq. (13)) blowing for at least 17 h over a minimum fetch of about 132 km (see Le Roux, 2009b). These waves would have a wavelength L_o of 39.03 m (Eq. (11)) and a height H_o of 1.38 m (Eq. (12)).

In deep water, both the median crest and trough diameters are half the wavelength L_o, i.e. 19.52 m. According to Eq. (9) or (10), at the surface ($z=0$) in a water depth of 100 m, the orbital velocity is 0.867 m s^{-1}, which decreases to 0.0155 m s^{-1} at a distance of 25 m from the surface and 0.0003 m s^{-1} at 50 m. The standard Airy (1845) equation $U_{oz} = \frac{\pi H_o}{T_w} e^{\left(\frac{-2\pi z}{L_o}\right)}$ gives the same results.

8.2. Intermediate and shallow water waves

Before calculating the characteristics of waves in any water depth, the breaking depth d_b and height H_b are required, which are obtained by iterating d in Eqs. (14) and (15). In the case of a fully developed 5 s wave breaking over a bottom slope of 1°, this yields $H_b = 1.68$ m and $d_b = 1.84$ m. The breaker length according to Eq. (16) is 25.64 m, whereas the median crest diameter is $\frac{L_o}{6} = 6.505$ m and the horizontal water particle velocity is 5.13 m s^{-1} (Eq. (9)). This equals the breaker celerity C_b given by $\frac{L_b}{T_w}$, as it should (Stokes, 1880; Miles, 1980).

Three equations to determine the breaking depth that also take account of the bottom slope are those of Collins (1970), Weggel (1972), and Komar (1998), which all require the breaker height. Taking H_b as 1.68 m and α as 1°, these equations yield breaking depths of 2.03, 2.05 and 1.03 m, respectively. Using the non-linear stream function theory of Dean (1965) to the 25th order (recommended for very shallow water conditions) with a wave period of 5 s, a height of 1.68 m and a damping factor of 0.3, breaking takes place at

a depth of 2.36 m. The average of these 4 equations is 1.87 m, thus agreeing reasonably well with 1.84 m obtained from Eqs. (14) and (15). According to the stream function theory, the wavelength reduces to 25.85 m at breaking (see http://www.coastal.udel.edu/faculty/rad/index.html), with a horizontal water particle velocity of 4.4 m s^{-1} in the wave crest. However, this does not coincide with the wave celerity of $\frac{25.85}{5} = 5.17 \, m s^{-1}$. Cnoidal theory, on the other hand (for a simplified methodology, see Le Roux, 2007b), yields a breaker length of 24.55 m compared to 23.79 given by an equation of Hedges (2009), but neither of these equations satisfies the condition that the horizontal water particle velocity in the wave crest must equal the wave celerity at breaking if MCD$_b$ is $\frac{L_o}{6}$ (see Le Roux, 2009a).

At an intermediate water depth of 10 m, the wavelength is 36.36 m according to Eqs. (16) and (17), whereas the height decreases to 1.23 m (Eq. (14)). For these conditions, linear wave theory predicts a wavelength of 36.61 m, compared to a length of 36.97 m given by 10th order stream function theory. The value of f increases to 2.0979 (Eq. (2)), so that η_t is -0.64 m (Eq. (3)). Cnoidal theory would calculate η_t to be -0.61 m below the SWL at this depth. (See Le Roux, 2008b, Appendix A). The median crest diameter decreases to 16.84 m (Eq. (4)), giving a horizontal water particle velocity of 1.08 m s^{-1} below the wave crest at the surface (Eq. (9)) and 0.33 m s^{-1} at the top of the boundary layer (Eq. (21)), which has a thickness of 0.05 m (Eq. (20)). The stream function theory yields a water particle velocity of 0.93 m s^{-1} at the surface and 0.29 m s^{-1} at the bottom below the wave crest in this case. At this depth the median trough diameter is 19.52 m (Eq. (5)), so that the horizontal water particle velocity would be 0.81 m s^{-1} at the surface and 0.24 m s^{-1} at the top of the boundary layer (Eq. (22)). The stream function theory calculates a velocity of 0.75 m s^{-1} at the surface and 0.29 m s^{-1} at the bottom below the wave trough. Stream function theory therefore makes no distinction between the boundary velocity under the wave crest and trough, respectively, in spite of the fact that it calculates the surface water particle velocity to be lower under the trough than under the crest.

Assuming well sorted sediments with a median size of 0.6 mm at the bottom, the critical boundary velocity is calculated by Eq. (23) at 0.28 m s^{-1} ($\rho = 1.025$ g cm^{-3}; $\mu = 0.0099$ g cm^{-1} s^{-1}; $s^* = 15.1886$; $C = 4.976$; $T_R = 1.7251$). Considering a bed roughness of 0.7 mm, the pivot angle is 32.6° (Eq. (29)) and the seaward critical velocity would be 0.28 m s^{-1} (subtracting the 1° seaward slope from 32.6° in Eq. (28)), compared to the landward critical velocity of 0.29 m s^{-1} (adding the landward slope of 1°). At this depth, only landward sediment entrainment will therefore take place. This is in accordance with the general observation that coastal accretion takes place during fair weather conditions. During storms, however, the seaward horizontal particle velocity under the wave trough will also exceed the critical boundary velocity of 0.28 m s^{-1}, and because the seaward water particle motion under the trough is of longer duration than the landward motion under the crest, net transport will be seaward, resulting in coastal erosion.

Similar calculations for a water depth of 3.6 m, where the waves will have trochoidal forms, show that the boundary layer increases to 0.18 m and the boundary velocity to 1.51 m s^{-1}. Quartz-density cobbles up to 54 mm could be entrained momentarily (Eqs. (23) and (27)), which is about the limit to which the latter equations have been tested in the laboratory (Le Roux, 2007c).

9. Conclusions

The main advantages of the proposed method, in comparison with existing models, can be summarized as follows:

— Previous wave theories are commonly applicable to certain depth ranges only and produce discrepant results with other theories in transitional zones. The theory discussed above uses the same

equations for all water depths and thus produces a seamless transition from deep water up to the breaking depth.

— Most methods to determine sediment entrainment under waves are based on linear wave theory, which cannot produce accurate results in shallow water. The method proposed here uses equations that are valid for both linear and non-linear waves.

— Previous methods to determine sediment entrainment under waves calculate only the critical and not the actual boundary velocity, and because they do not take the water depth into account, cannot be used in different water depths. The proposed model calculates both the critical and actual conditions and can therefore be used to predict entrainment from deep water up to breaking depth.

— The thickness of the boundary layer can be computed from the modeled wave conditions and thus eliminates the need to physically measure the boundary velocity, which is difficult to do under field conditions.

— Sediment entrainment can be determined under both the wave crest and trough, where the horizontal particle velocity can differ considerably in shallow water. This paves the way for the prediction of net seaward or landward transport under various wave and bottom slope conditions.

Acknowledgements

Appendix A. List of symbols

A_{wl}	horizontal water particle displacement at top of boundary layer
A_{whz}	horizontal water particle displacement at depth z from DWL
A_{wvz}	vertical water particle displacement at depth z from DWL
d	water depth with respect to SWL
D	sediment grain size
D_1	bed roughness grain size
D_2	transported sediment grain size
DWL	displaced water level
g	acceleration due to gravity
H	wave height
L	wavelength
MCD	median crest diameter
MTD	median trough diameter
Subscript $_b$	condition at breaking
Subscript $_o$	condition in deep water
Subscript $_w$	condition in any water depth
Subscript $_c$	condition under wave crest
Subscript $_t$	condition under wave trough
SWL	still water level
s_*	scaled dimensionless immersed sediment weight
T_w	wave period
U_a	wind velocity at 10 m above SWL
U_{wl}	boundary velocity
U_{wle}	critical boundary velocity
U_{whz}	horizontal water particle velocity at depth z from SWL
y_c	distance of wave crest from bottom
y_t	distance of wave trough from bottom
z	depth below DWL
α	bottom slope (degrees)
δ	boundary layer thickness
μ	dynamic viscosity
υ	kinematic viscosity
η_t	distance of wave trough below SWL
ρ	water density
ρ_s	grain density
ρ_γ	submerged grain density
φ	grain pivot (friction) angle

References

Airy, G.B., 1845. Tides and waves. Encyclopedia Metropolitan 192, 241–396.

Allen, J.R.L., 1982. Simple models for the shape and symmetry of tidal sand waves: 1. Statistically-stable equilibrium forms. Marine Geology 48, 31–49.

Bagnold, R.A., 1946. Motion of waves in shallow water. Interaction of waves and sand bottoms. Proceedings of the Royal Society, Ser. A: Mathematical Physical and Engineering Sciences 187, 1–15.

Boussinesq, J., 1871. Theorie de l'intumescence liquide appelee onde solitaire ou de translation se propageant dans un canal rectangulaire. Comtes Rendus de l`Académie des Sciences Paris 72, 755–759.

Bretschneider, C.L., 1960. A theory for waves of finite height. Proc. 7th Coastal Engineering Conference, vol. 1, pp. 146–183.

Chakrabarti, S.K., 1987. Hydrodynamics of Offshore Structures. WIT Press, Southampton, U.K.

Chappelear, J.E., 1962. Shallow water waves. Journal of Geophysical Research 67, 4693–4704.

Cokelet, E.D., 1977. Steep gravity waves in water of arbitrary uniform depth. Philosophical Transactions of the Royal Society of London, Series A, Mathematical Physical and Engineering Sciences 286, 183–230.

Collins, I.A., 1970. Probability of breaking wave characteristics. Proc. 12th Conference of Coastal Engineering. ASCE, pp. 399–414.

Dean, R.G., 1965. Stream function representation of nonlinear ocean waves. Journal of Geophysical Research 70, 4561–4572.

Dean, R.G., Dalrymple, R.A., 1991. Water Wave Mechanics for Engineers and Scientists. World Scientific Pub. Co, Teaneck, N.J.

Dyer, K.R., 1986. Coastal and Estuarine Sediment Dynamics. Wiley, Chichester. 342 pp.

Fenton, J.D., 1985. A fifth-order Stokes theory for steady waves. ASCE Journal of Waterways, Port, Coastal and Ocean Engineering 111, 216–234.

Fenton, J.D., 1988. The numerical solution of steady water wave problem. Journal of Comparative Geosciences 14, 357–368.

Hammond, T.M., Collins, M.B., 1979. On the threshold of transport of sand-sized sediment under the combined influence of unidirectional and oscillatory flow. Sedimentology 26, 795–812.

Hedges, T.S., 2009. Discussion of "A function to determine wavelength from deep into shallow water based on the length of the cnoidal wave at breaking" by J.P. Le Roux. Coastal Engineering 56, 94–95.

Ippen, A.T., 1966. Estuary and Coastline Hydrodynamics. McGraw-Hill Book Co., New York.

Jonsson, I.G., 1966. On the existence of universal velocity distribution in an oscillatory turbulent boundary layer. Coastal Engineering Laboratory, Technical University of Denmark, Copenhagen. Basic Research Progress Report 12, 2–10.

Komar, P.D., 1998. Beach Processes and Sedimentation. Prentice Hall, Upper Saddle River, N.J.. 543 pp.

Komar, P.D., Miller, M.C., 1973. Sediment threshold under oscillatory water waves. Journal of Sedimentary Petrology 43, 1101–1110.

Komar, P.D., Miller, M.C., 1975. On the comparison between the threshold of sediment motion under waves and unidirectional currents with a discussion on the practical evaluation of the threshold. Journal of Sedimentary Petrology 45, 362–367.

Korteweg, D.J., De Vries, G., 1895. On the change in form of long waves advancing in a rectangular channel, and on a new type of stationary waves. Philosophical Magazine, 5th Series 39, 422–443.

Latoine, E.V., 1960. The second approximation to cnoidal and solitary waves. Journal of Fluid Mechanics 19, 430–444.

Latoine, E.V., 1962. Limiting conditions for cnoidal and Stokes waves. Journal of Geophysical Research 67, 1555–1564.

Latoine, E.V., 1965. Series solutions for shallow water waves. Journal of Geophysical Research 70, 995–998.

Leeder, M., 1999. Sedimentology and Sedimentary basins: From Turbulence to Tectonics. Blackwell Science, Oxford. 592 pp.

Le Roux, J.P., 2001. A simple method to predict the threshold of particle transport under oscillatory waves. Sedimentary Geology 143, 59–70.

Le Roux, J.P., 2005. Grains in motion: a review. Sedimentary Geology 178, 285–313.

Le Roux, J.P., 2007a. A simple method to determine breaker height and depth for different deepwater height/length ratios and sea floor slopes. Coastal Engineering 54, 271–277.

Le Roux, J.P., 2007b. A function to determine wavelength from deep into shallow water based on the length of the cnoidal wave at breaking. Coastal Engineering 54, 770–774.

Le Roux, J.P., 2007c. A unified criterion for initiation of sediment motion and inception of sheet flow under water waves—discussion. Sedimentology 54, 1447–1448.

Le Roux, J.P., 2008a. An extension of the Airy theory for linear waves into shallow water. Coastal Engineering 55, 295–301.

Le Roux, J.P., 2008b. Profiles of fully developed (Airy) waves in any water depth. Coastal Engineering 55, 701–703.

Le Roux, J.P., 2009a. Characteristics of developing waves as a function of atmospheric conditions, water properties, fetch and duration. Coastal Engineering 56, 479–483.

Le Roux, J.P., 2009b. "A function to determine wavelength from deep into shallow water based on the length of the cnoidal wave at breaking"—reply to discussion by T.S. Hedges. Coastal Engineering 56, 96–97.

Li, H., 1954. Stability of oscillatory laminar flow along a wall. Beach Erosion Board, Technical Memo 47, 48 pp.

Manohar, M., 1955. Mechanics of bottom sediment movement due to wave action. Beach Erosion Board. Technical Memo 75.

Mei, C.C., 1991. The Applied Dynamics of Ocean Surface Waves. World Scientific Pub. Co., Teaneck, N.J.

Middleton, G.V., Southard, J.B., 1984. Mechanics of sediment movement, 2nd ed. : Lecture Notes for Short Course, vol. 3. Society of Economic Paleontologists and Mineralogists, Rhode Island. 400 pp.

Migniot, C., 1977. Action des courants, de la houle et du vent sur les sediments. La Houille Blanche 1 (1997), 9–47.

Miles, J.W., 1980. Solitary waves. Annual Reviews of Fluid Mechanics 12, 11–43.

Peregrine, D.H., 1972. Equations for water waves and the approximation behind them. In: Meyer, E.E. (Ed.), Waves on Beaches and Resulting Sediment Transport. Academic Press, pp. 95–121.

Phillips, O.M., 1977. The Dynamics of the Upper Ocean, 2nd Ed. Cambridge University Press, Cambridge.

Rance, P.J., Warren, N.F., 1969. The threshold of movement of coarse material in oscillatory flow. Proceedings of the 11th Coastal Engineering Conference. ASCE, New York, pp. 487–491.

Shore Protection Manual, 1984. 4th Ed. U.S. Army Engineer Waterways Experimental Station, vol. 2. Government Printing Office, Washington, D.C.

Skjelbreia, L., Hendrickson, J., 1961. Fifth order gravity wave theory. Proceedings of the 7th Coastal Engineering Conference, vol. 1, pp. 184–196.

Soulsby, R.L., Whitehouse, R.J.S., 1997. Threshold of sediment motion in coastal environments. Pacific Coasts and Ports '97, 13th Australian Coastal and Engineering Conference and 6th Australian Port and Harbour Conference, 1997, Christchurch, New Zealand. HR Wallingford, Oxon, pp. 149–154.

Stokes, G.G., 1880. Mathematics and Physics Papers, vol. 1. Cambridge Univ. Press, Cambridge.

Van Dyke, M., 1982. An Album of Fluid Motion. Parabolic Press, Stanford, CA.

Van Rijn, L.C., 2007. Unified view of sediment transport by currents and waves 1: initiation of motion, bed roughness and bed-load transport. Journal of Hydraulic Engineering, ASCE 133 (6), 649–667.

Wang, Y.-H., 2007. Formula for predicting bedload transport rate in oscillatory sheet flows. Coastal Engineering 54, 594–601.

Weggel, J.R., 1972. Maximum breaker height. Journal of Waterways and Harbors, Coastal Engineering Division 98, 529–548.

White, T.E., 1989. Using sediment-threshold theories in waves and currents. Proceedings of the International Symposium on Sediment Transport Modeling. ASCE, New York, pp. 248–253.

Whitehouse, R.J.S., Hardisty, J., 1988. Experimental assessment of two theories for the effect of bedslope on threshold of bedload transport. Marine Geology 79, 135–139.

You, Z.J., Yin, B., 2006. A unified criterion for initiation of sediment motion and inception of sheet flow under water waves. Sedimentology 53, 1181–1190.